Proceedings of IPC'02
2002 ASME International Pipeline Conference
September 29 - October 3, 2002, Calgary, Alberta, Canada

IPC02-27099

THE EFFECT OF THE SLIP VELOCITY ON THE DIFFERENTIAL PRESSURE IN MULTIPHASE VENTURI FLOW METERS

Emilio E. Paladino

Computational Fluid Dynamics Laboratory
Department of Mechanical Engineering
Federal University Santa Catarina
Florianopolis - SC Brazil. CEP 88040-900
E-mail: emilio@sinmec.ufsc.br

Clovis R. Maliska

Computational Fluid Dynamics Laboratory
Department of Mechanical Engineering
Federal University Santa Catarina
Florianopolis - SC Brazil. CEP 88040-900
E-mail: maliska@sinmec.ufsc.br

ABSTRACT

Venturi tubes and orifice plates are devices largely used in the petroleum industry for measuring multiphase flows. In the project and calibration of these flow meters, the homogeneous model is commonly used. This model calculates the velocity and pressure drop of the mixture using correlations for single phase flow with a modified viscosity and density to account for the presence of the other phase, but no consideration is made about the relative velocity between the phases. However, the pressure difference, the measuring variable in these flow meters, is known to be affected by the relative velocity between phases, which becomes more and more important when the flow mixture accelerates. This paper addresses this issue and aims to demonstrate the importance of using models which consider the relative velocity between phases in the calculation of the flow within a venturi meter. For this purpose, pressure-difference values obtained using the two-fluid model based on an Eulerian - Eulerian approach for the multiphase flow are compared with the results of the homogeneous model and with experimental data. Both theoretical calculations are performed using the CFX4.4 package, code which solves multidimensional multiphase flows. Considerations about the two-fluid model are presented, focusing, on the effects of the stress tensor in the dispersed phase. Considerations regarding the two-dimensional nature of the flow are also made. Test cases are presented in order to determine the dependency of the differential pressure with void fraction and slip velocity.

NOMENCLATURE

i, j Indicates phase i and j
I Indicates interface
g Gravity acceleration
r_i Volumetric Fraction of phase i
$\mathbf{U}_i$ Velocity of phase i
$\mathbf{T}_i$ Stress Tensor of phase i
$\mathbf{M}_{iI}$ Interfacial momentum transfer term
X_i Phase indicator function

INTRODUCTION

Pipeline transport of multiphase mixtures is commonly encountered in the petroleum industry. Mixtures of oils, water and gas produced from wells or condensate fractions flowing with gas in gas pipeline transport are common examples. The accurate flow rate measurement of such multiphase flows is extremely important in areas like pipeline management, leak detection, and fiscal metering. Unlike the measurement of single phase flows using differential pressure meters, the multiphase flow behavior poses difficulties for the accurate measurement.

Differential pressure flow meters are present in several measurement systems as,for example, in the one described by Mehdizadeh & Farchy (1995). This system encompasses a volumetric flow meter, two venturi tubes and a water cut meter. The two venturi meters are supposed to measure the two velocities, one for each phase. Another system using a venturi as veloc-

ity meter is that described by Boyer & Lemonnier (1996) which include a Venturi and a mixer to homogenize phase velocities. Whatever the application, Venturi type flow meters are largely used in pipeline transport of hydrocarbons due to their simplicity, low cost, robustness and maintainability. These characteristics are strongly required for field applications, specifically in off-shore conditions.

In differential pressure-type flow meters, the accuracy of the flow measurement depends strongly on the knowledge of the flow behavior, specially on the relation between differential pressure and the mean velocity of the flow. This relation is affected by various flow parameters like void fraction, relative velocity between phases (slip velocity), interfacial momentum transfer etc.

The main objective of this paper is to present the application of a two dimensional two-fluid model for the study of the flow structure in bubbly regime within a Venturi, focusing in the influence of the slip velocity on the relation between pressure-difference and flow-rate.

MATHEMATICAL MODELLING

In correlating pressure drop in multiphase venturi meters, it is commonly used the homogeneous model. This model is similar to a single phase model, in the sense that it considers only one velocity field, but uses special fluid properties, called properties of the mixture, to represent the multiphase flow behavior. Since the total mass flow rate is equal to the sum of the individual mass flow rates of each phase,

$$\rho_{mix}\mathbf{U}_{mix} = \rho_{liq}r_{liq}\mathbf{U}_{liq} + \rho_{gas}r_{gas}\mathbf{U}_{gas} \tag{1}$$

the density of the mixture can be obtained as

$$\rho_{mix} = \rho_{liq}r_{liq} + \rho_{gas}r_{gas} \tag{2}$$

which, obviously, considers that both velocities are equal, the main simplificative hypothesis of the homogeneous model. Summing up the momentum equations for each phase in the two-fluid model[1] and considering again the equality of the velocities, one obtains a viscosity for the mixture as

$$\mu_{mix} = \mu_{liq}r_{liq} + \mu_{gas}r_{gas} \tag{3}$$

This viscosity appears naturally when it is considered that the phase velocities are the same. In order to improve the model, several other correlations for the viscosity are presented in the literature (see for example Collier & Thome (1995, cap. 2)). In this work, the above model will be used when we refer to the homogeneous model.

The two-fluid model

The two-fluid model considers one velocity field for each phase. In this model each phase is supposed to behave as a continuous media occupying the entire domain where the amount of each phase present is given by the volumetric fraction. The governing equations for this model are derived by averaging the local conservation equations for each phase, together with their corresponding conservation equations at the interfaces, *i.e.*, the jump conditions. The mass and momentum conservation equations for the two-fluid model are, then, given by,

$$\frac{\partial}{\partial t}(r_i\rho_i) + \nabla\cdot(r_i\rho_i\mathbf{U}_i) = 0 \tag{4}$$

$$\frac{\partial}{\partial t}(r_i\rho_i\mathbf{U}_i) + \nabla\cdot(r_i(\rho_i\mathbf{U}_i\mathbf{U}_i - \mathbf{T}_i + \mathbf{T}_i^{Turb}) = -r_i\nabla p_i + \\ +(p_{iI} - p_i)\nabla r_i + \mathbf{M}_{iI} + \sum_{j=1}^{N_P}(\dot{m}_{ij}\mathbf{U}_j - \dot{m}_{ji}\mathbf{U}_i) + r_i\mathbf{f} \tag{5}$$

where subindex i indicates the phase, $\mathbf{M}_{iI}$ is the interface transport term, r_i is the volumetric fraction of phase i and $\dot{m}_{ji}$ is the mass transferred from phase j to i. A full description of the derivation of these equations is presented by Drew (1983).

The term $(p_{iI} - p_i)$ contains the force due to the interfacial pressure distribution. In vertical flows this term represents the buoyancy force as this force is given by pressure (hydrostatic) differences distribution at the interfaces. Actually , the interfacial pressure of all phases is considered equal and the buoyancy force is calculated by $\mathbf{F}_B = (\rho_{liq} - \rho_{gas})V_{bubble}\mathbf{g}$. It is assumed that the bulk pressure of all phases, in the presence of any flow disturbance, have instantaneous equalization. Therefore, the pressure of the mixture in all points (phases and interfaces) is considered equal. As this problem does not include phase transition, the term $\sum_{j=1}^{N_P}(\dot{m}_{ij}\mathbf{U}_j - \dot{m}_{ji}\mathbf{U})$ is also zero.

For the continuous phase, a $k-\varepsilon$ turbulence model was used, including the bubble induced turbulence through Sato & Sekoguchi (1975) model. For the dispersed phase, the viscous terms were neglected, since in the authors judgement, it is not available in the literature physically founded models for the stress tensor. Drew (1983) shows that the effective viscosity of the dispersed phase could be obtained multiplying the effective viscosity of the continuous phase by the density ratio as,

[1] See the next section

$$\mu_{gas}^{eff} = \frac{\rho_{gas}}{\rho_{liq}} \cdot \mu_{liq}^{eff} \quad (6)$$

For high density ratios, as in this case, the stress terms for the dispersed phase can be neglected. However, this assumption has no physical basis. In solid-gas flows, since the disperse phase concentrations are high with strong interactions between particles, it is common to use the kinetic theory of granular flow based on an analogy with the kinetic theory of gases (see for example Enwald et al. (1996)). For the case of bubbly flows, there is no such analogy as the bubble interactions, which include bubble deformation, breaking-up and coalescence, are much more complex. Another reason for neglecting the bubble interactions is based on the physical phenomenology. It is known that viscous term arrives from the interaction of fluid layers. For low void fractions (as is the case of bubbly regime) the interaction between the bubbles is weak and no shear tension arrives for the dispersed phase. Finally, the viscous dissipation within the bubble is transferred to the continuous phase by correct modelling the interfacial force. Figure 1 illustrates this.

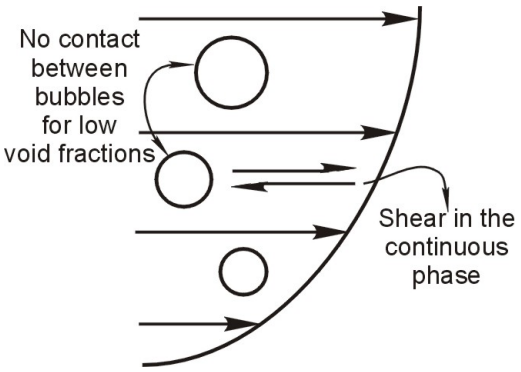

Figure 1. SHEAR STRESSES FOR CONTINUOUS AND DISPERSED PHASES.

In the CFX4 code the viscous terms in the dispersed phase are neglected by setting a very low viscosity ($\mu = 1e-20$) and setting a slip condition at the wall boundaries for this phase.

Then, the momentum balance for the dispersed phase is given by the inertial, pressure, interfacial and body forces as is done in several one-dimensional models present in the literature (Lewis & Davidson (1985), Cout et al. (1991), Kowe et al. (1988), among others).

The homogeneous model

This simple model can be deduced from the more general two-fluid model by summing over all phases the conservation equations. The main disadvantage of this model is that it considers only one velocity field for all phases. For the problem we are interested in, *i.e.*, to predict multiphase flow field in geometries like Venturis and orifice plates, where high local accelerations are present, generating high slip velocities, this assumption is no longer valid. The governing equations for this model are similar to those for single phase flows, but uses special fluid properties representing the mixture behavior, as described above. The CFX4 code allows to calculate the volumetric fractions for each phase by solving individual mass conservation equations and one momentum equation for all phases. These equations are,

$$\frac{\partial}{\partial t}(r_i\rho_i) + \nabla \cdot (r_i\rho_i\mathbf{U}_i) = 0 \quad (7)$$

$$\frac{\partial}{\partial t}(\rho_{mix}\mathbf{U}) + \nabla \cdot ((\rho_{mix}(\mathbf{UU}) - \mathbf{T}_{mix} + \mathbf{T}_{mix}^{Turb}) = -\nabla p + \mathbf{f} \quad (8)$$

where ρ_{mix} is given by Eq. 2. The stress tensor for the mixture is calculated by the traditional approach, that is, proportional to the strain tensor, but using a mixture viscosity given by Eq. 2. For very fine dispersions, as oil in water emulsions, the hypothesis of the homogeneity of velocities is valid and this model could be used. Care should be exercised, however, when the mixture shows non-newtonian behavior. The velocity in the previous equations represents the velocity of the center of mass of the mixture and is given by,

$$\mathbf{U} = \frac{1}{\rho_{mix}} \sum_{i=1}^{N_P} r_i\rho_i\mathbf{U}_i \quad (9)$$

Interfacial forces

The interfacial forces arrives from the phase interactions through the interface. These forces, represented by the term $\mathbf{M}_{iI}$ in Eq. 5, are the integration of all momentum exchanges at the interface. When no phase transition is present, these force are due to pressure and viscous stresses at the interface, given by

$$\mathbf{M}_{iI} = \langle (p - p_{iI})\nabla X_i - T_{iI}\nabla X_i \rangle \quad (10)$$

As for the two-fluid model, it is considered that pressure reaches instantaneous equilibrium, then $p_i = p_{iI}$ (see Drew

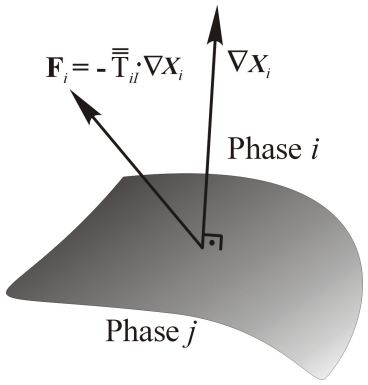

Figure 2. LOCAL INTERFACIAL FORCE.

(1983)). Furthermore, as superficial tension can be neglected, $p_{jI} = p_{iI}$, the pressure for the whole mixture is equal and,

$$\mathbf{M}_{iI} = \langle -T_{iI} \nabla X_i \rangle \tag{11}$$

where the function X_i is called phase indicator and is defined as,

$$X_i(\mathbf{r},t) = \begin{cases} 1 & \text{if } \mathbf{r} \in \text{phase } i \\ 0 & \text{otherwise} \end{cases} \tag{12}$$

and its gradient is normal to the interface pointing outward. Figure 2 shows schematically the local interfacial force which, after integration, gives the total momentum transfer across the interface.

As the averaged equations do not provide knowledge about flow details, constitutive equations are needed for the calculation of interfacial momentum transfer. The correct understanding of the origin of the interfacial momentum transfer is important in order to deduce consistent constitutive relations. For dispersed flows, these terms arrives from the forces acting in a particle submerged in a rotating straining viscous flow. From this general approach several forces appear due to different phenomena. The forces commonly considered in the models are:

Drag Force This force arrives from the unsymmetrical pressure distribution around the particle and due to skin friction. All these effects are considered in a drag coefficient with the force given by

$$\mathbf{M}_{iI}^D = \frac{1}{2} C_D \rho_i A |\mathbf{U}_j - \mathbf{U}_i| (\mathbf{U}_j - \mathbf{U}_i) \tag{13}$$

where i represents the continuous phase and A the projected area of the particle.

Virtual Mass Force This force is due to the relative acceleration between phases. It is known that when a particle passes through a fluid at rest, a volume of fluid, proportional to the particle volume, is displaced and assumes the particle velocity. The acceleration from the rest to the particle velocity (or from the continuous phase velocity to the dispersed phase velocity, in the case of two-phase flows), originates a force given by,

$$\mathbf{M}_{iI}^{VM} = \rho_i r_j C_{VM} \left(\frac{D_j \mathbf{U}_j}{Dt} - \frac{D_i \mathbf{U}_i}{Dt} \right) \tag{14}$$

where C_{VM} represents the fraction of the particle volume displaced from the continuous phase. For an infinite medium $C_{VM} = 0.5$, and this value can be used for low void fractions.

Lift Force This force is perpendicular to the main flow and is originated by the vorticity of the continuous phase. It is given by,

$$\mathbf{M}_{iI}^L = r_j \rho_i C_L (\mathbf{U}_j - \mathbf{U}_i) \cdot (\mathbf{U} \times \vec{\omega}) \tag{15}$$

For more details about the physical significance of the virtual mass and lift forces, see, for example, Drew (1983) or Kowe et al. (1988).

In this work, only the drag force has been considered. Although the non-drag forces represent a small fraction of the interfacial momentum transfer term $\mathbf{M}_{iI}$, for various applications (strong local accelerations is one example), these forces can play an important role. As will be seen in the next section, not considering the virtual mass force does not affect significantly the velocity fields, but can greatly underestimate the determination of the differential pressure, the focus of this study.

Various models exist for the drag coefficient, depending on the local flow regime around the bubble. Here, it was used a model based on a terminal bubble velocity, which takes into account the bubble deformation for high velocity regimes. An expression for the drag coefficient is obtained by invoking the equilibrium between buoyancy and drag forces for a bubble ascending in a quiescent liquid, as

$$(\rho_{liq} - \rho_{gas}) g \frac{4}{3} \pi r^3 = C_D \pi r^2 \frac{1}{2} \rho_{liq} U_T^2 \tag{16}$$

which gives,

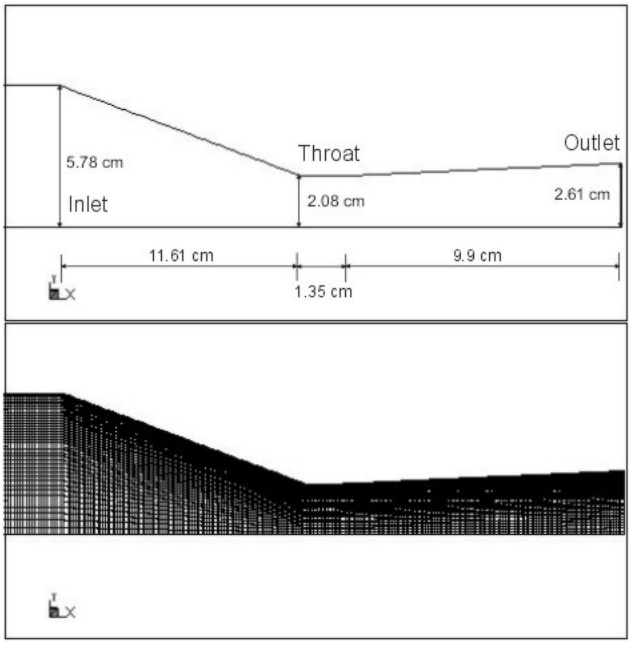

Figure 3. GEOMETRY USED BY Kuo & Wallis (1988) AND COMPUTATIONAL GRID USED IN THIS WORK

$$C_D = \frac{8}{3}\frac{gr\Delta\rho}{\rho_{liq}U_T^2} \tag{17}$$

where U_T is the terminal bubble rise velocity, g is the gravity acceleration an r is the bubble radius. In all cases the bubble mean diameter used was 5 mm and terminal rising velocity of 0.2 m/s, giving $C_D = 1.63$. Further studies are being carried out to investigate the influence of bubble diameter and break-up and coalescence in the differential pressure values and flow structure.

RESULTS

In this section some results calculated using the package CFX4.4 are shown. As was mentioned, this code solves the two-fluid model in three dimensions. Velocity fields were compared with experimental data of Kuo & Wallis (1988) and differential pressure values with the data presented by Lewis & Davidson (1985). Kuo & Wallis (1988) measured the velocity of a single bubble in a Venturi tube using an optical system and the water velocities (continuous phase) using a pitot tube.

Figure 3 shows the geometry used by Kuo & Wallis (1988) and the computational grid used in the present work.

The problem was treated as two-dimensional, using the symmetry condition at the centerline. Some tests were made using a three dimensional geometry and no differences were found in terms of flow structure and velocity distributions. The two-dimensional results obtained were averaged through the cross section of the Venturi in order to compare with one-dimensional results given by Kuo & Wallis (1988). For a generic scalar ϕ which could represent velocity components, pressure or void fraction, the average value at any point of the axial coordinate is,

$$\bar{\phi} = \frac{1}{A}\int_{CL}^{Wall} \phi dA \tag{18}$$

Figures 4 and 5 shows a comparison of average velocities along the Venturi axis obtained using the two-fluid model and the results of Kuo & Wallis (1988) for inlet velocities of 0.5 m/s and 0.7 m/s respectively. These velocities correspond to that of the liquid at the inlet section. To ensure that the fully developed flow at the Venturi inlet is reached, the simulation domain is expanded upstream to the Venturi inlet. Then, at this point, the gas phase velocity, set equal to the liquid velocity at the domain entrance, reaches he liquid velocity plus the terminal velocity U_T

At the convergent section, there are small differences, probably within the experimental uncertainty. The differences observed at the divergent part, mainly for the bubbles velocities, could be due to the increasing effects of turbulence in this section. Furthermore, the lift force (transversal to the main flow) increased due to vorticity raise at this section, tends to deviate the bubbles from its trajectory, causing strong velocity fluctuations. In this case the two dimensional effects are important and

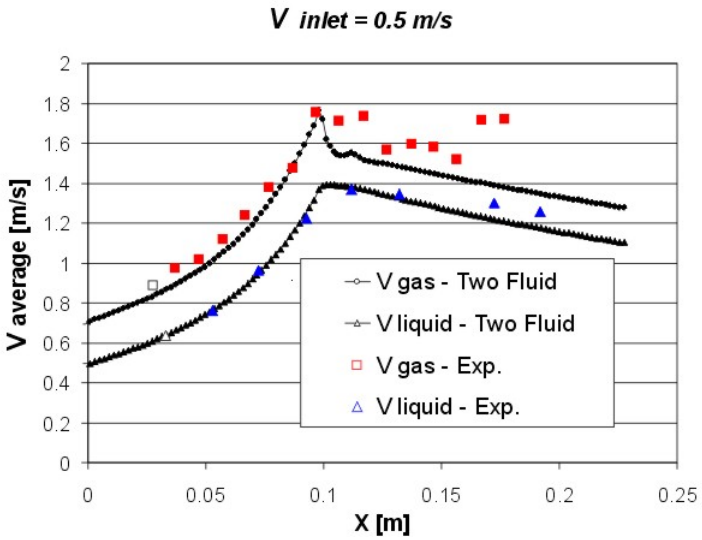

Figure 4. AIR AND WATER AVERAGED VELOCITIES ALONG THE VENTURI COMPARED WITH EXPERIMENTAL DATA OF KUO & WALLIS (1988). $V_{Inlet} = 0.5m/s$

the velocity of one bubble (measured by Kuo & Wallis (1988)) could not represent the velocity field of the dispersed phase.

Figure 6 shows the geometry used by Lewis & Davidson (1985) and the grid used in the present work. Again, the symmetry condition was used to save computer time. Since in this case the cross section is circular, the axi-symmetric conditions were used.

Figures 7 and 10 show the differential pressure measured between pressure taps shown in Fig. 6 and the results obtained using the Homogeneous and Two-Fluid models, for superficial liquid velocities of 0.54 m/s and 0.65 m/s, respectively.

Considerable differences can be seen for high void fractions between experimental and the calculated differential pressure values, even using the two-fluid models. Probably these differences are due to the non consideration of the virtual mass forces. As explained, these forces take into account that a parcel of continuous phase (virtual mass) assumes the bubble velocity and, therefore, accelerates with the bubble. In highly accelerated flows, the case of venturi and orifice meters, the increase in acceleration of a high density fluid (water) would require a higher pressure gradient. Boyer & Lemonnier (1996) also compared their results using the three field model due to Kowe et al. (1988), with the experimental results obtaining errors less than 4 %. In this model the three fields are the bubbles, the liquid far from the bubbles and the liquid displaced by bubbles, which takes the bubble velocity. This is a more consistent treatment for taking into account the effect described above. The authors believe that using a correct form of the virtual mass force, the two-fluid model is effective for correct predicting the differential pressure. Further efforts are being made in order to study the influence of such forces in the differential pressure calculations using the two-fluid model.Another feature of the model used here is the consideration of the two-dimensionality of the flow.

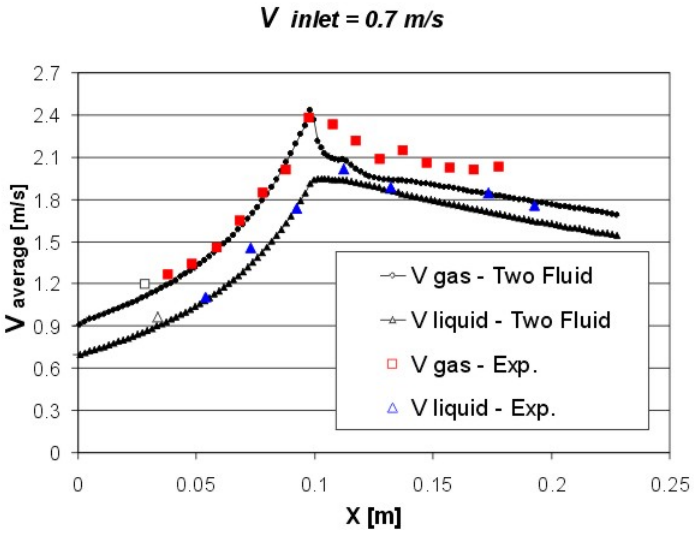

Figure 5. AIR AND WATER AVERAGED VELOCITIES ALONG THE VENTURI COMPARED WITH EXPERIMENTAL DATA OF KUO & WALLIS (1988). $V_{Inlet} = 0.7m/s$

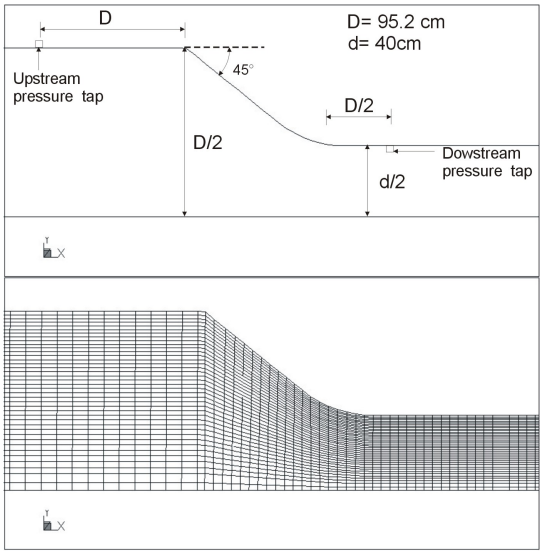

Figure 6. GEOMETRY USED BY LEWIS & DAVIDSON (1985) AND GRID USED IN THE PRESENT WORK

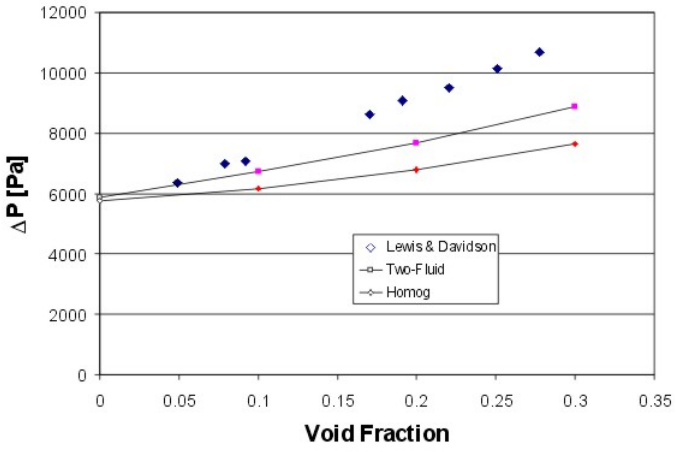

Figure 7. COMPARISON BETWEEN HOMOGENEOUS AND TWO-FLUID MODEL WITH EXPERIMENTAL DATA OF LEWIS & DAVIDSON (1985) FOR LIQUID SUPERFICIAL VELOCITY OF 0.54 m/s

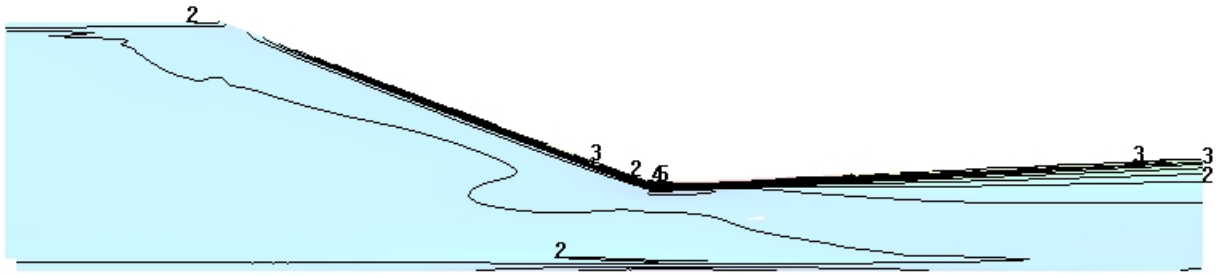

Figure 8. VOID FRACTION DISTRIBUTION IN A VENTURI WITH INLET VELOCITY AND VOID FRACTION OF 0.5 m/s AND 20 % RESPECTIVELY

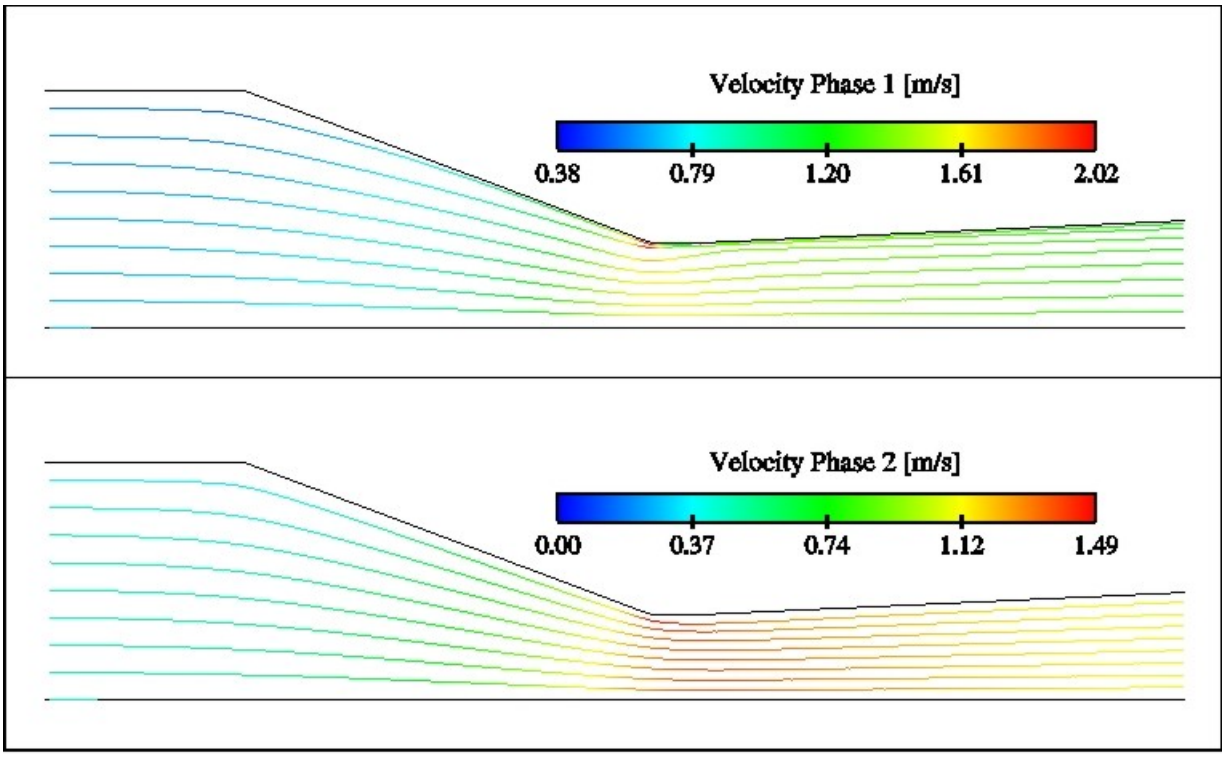

Figure 9. TRAJECTORIES OF BUBBLES (ABOVE) AND LIQUID PARTICLES (BELOW) IN A VENTURI WITH INLET VELOCITY AND VOID FRACTION OF 0.5 M/S AND 20 % RESPECTIVELY

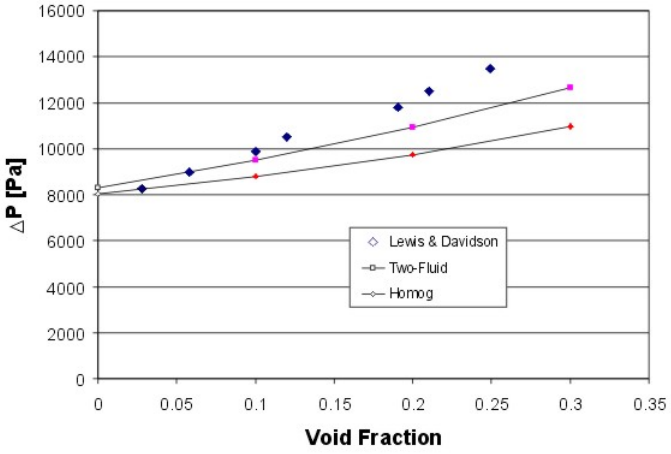

Figure 10. COMPARISON BETWEEN HOMOGENEOUS AND TWO-FLUID MODEL WITH EXPERIMENTAL DATA OF LEWIS & DAVIDSON (1985) FOR LIQUID SUPERFICIAL VELOCITY OF 0.65 m/s

Figure8 shows the predicted void fraction distribution in the Venturi shown in the Figure 3 for an inlet liquid velocity and void fraction of 0.5 m/s and 20% respectively.

As could be seen, there is high gas concentration near walls, in particular at the throat, region where the pressure transducer would be located. This fact could lead to gas entering into the device, causing, for example, a leak detection system instability. Figure 9 shows the streak lines for the gas (above) and for liquid. It can be seen that bubbles tend to concentrate in the wall regions at the throat, generating high void fraction in this region.

These results show that, besides the differential pressure calculations used for metering, it is of great interest to know the two-dimensional characteristics of the flow in the designing process of a differential pressure-type flow meter.

CONCLUSIONS

Several results were presented using the two-fluid model and compared with the homogeneous model and experimental data. For the differential pressure calculation, the two-fluid model shows to be better than the homogeneous model, commonly used in practical calculations, but the values are still far from the experimental data. This requires further improvements of the model, in particular of the interfacial forces. In this respect, efforts are being made in order to improve the two-fluid model, since this will lead to a simpler model with better numerical stability characteristics.

The two-dimensional structure of the flow was also considered in the paper. The knowledge of gas and liquid distribution is of fundamental importance in the designing of metering systems.

ACKNOWLEDGMENT

This work was realized with the financial support of the Brazilian National Petroleum Agency - ANP and of Financier of projects and studyes - FINEP, through Human Resources Program of ANP for Petroleum and Natural Gas.

REFERENCES

Boyer, C., Lemonnier, H., 1996. Design of a flow metering process for two-phase dispersed flows. International Journal of Multiphase Flows 22 (4), 713–732.

Collier, J. G., Thome, J. R., 1995. Convective Boiling and Condensation. Oxford Science Publications, Walton St., Oxford OX2 6DP.

Cout, B., Brown, P., Hunt, A., 1991. Two phase bubbly-droplet flow thought a contraction: Experiments and a unified model. International Journal of Multiphase Flows 17 (3), 291–307.

Drew, D. A., 1983. Mathematical modelling of two-phase flows. Annual Review of Fluid Mechanics 15 (4), 261–291.

Enwald, H., Peirano, E., Almstedt, A. E., 1996. Eulerian two-phase theory applied to fluidization. International Journal of Multiphase Flows 22, 21–66.

Kowe, R., Hunt, J. C., Hunt, A., Couet, B., Bradbury, L. J., 1988. The effects of bubbles on the volume fluxes and the pressure in unsteady and non-uniform flow of liquids. International Journal of Multiphase Flows 14 (5), 587–606.

Kuo, J. T., Wallis, G. B., 1988. Flow of bubbles through nozzles. International Journal of Multiphase Flows 14 (5), 547–564.

Lewis, D. A., Davidson, J. F., 1985. Pressure drop for bubbly gas-liquid flow through orifice plates and nozzles. Chem. Eng. Res. Des. 63, 149–156.

Mehdizadeh, P., Farchy, D., 1995. Multi-phase flow metering using dissimilar flow sensors: theory and field trial results. SPE Paper (29847), 59–72.

Sato, Y., Sekoguchi, K., 1975. Liquid velocity distribution in two-phase bubble flow. International Journal of Multiphase Flows 2, 79.